INVESTIGATING THE RESPONSE OF AN OPERATIONAL SNOWMELT MODEL TO UNUSUAL SNOW CONDITIONS AND MELT DRIVERS

Mark S. Raleigh[1] and Jeffrey S. Deems[1]

ABSTRACT

In the mountainous western United States, operational runoff forecasting centers typically use streamflow observations to calibrate coupled snow-hydrology models over multi-decadal periods. When seasonal or annual snow conditions deviate from mean historic conditions, such as with extreme events (e.g., snow drought) or hydrologic disturbances (e.g., dust-on-snow), the accuracy of operational models can degrade. Recently, streamflow forecasting errors in the Upper Colorado River Basin (UCRB) have been linked to interannual variations in dust radiative forcing, as retrieved from remote sensing. Here we build off previous work in the UCRB to quantify spatial and temporal variations in optimal operational snow model parameters and evaluate linkages with interannual variations in snow accumulation (e.g., low vs. high snow years), spring snowstorm regime, spring temperature, and dust radiative forcing. Using 30 years of snow pillow data and corrected air temperature data at 110 stations in the Colorado-Utah-Wyoming domain, we derive optimal snow model parameters with independent calibrations at each site and year. Results show coherent spatial and temporal patterns in the model melt factors that are most strongly linked to peak snow accumulation and dust-on-snow. These results have implications for operational forecasting, which uses fixed snow model parameters, irrespective of normality in snow conditions. (KEYWORDS: operational snow model, melt factors, snow accumulation, dust-on-snow, Upper Colorado River Basin)

INTRODUCTION

Snowmelt is the dominant source of streamflow for many mountainous watersheds in the western United States, such as the Colorado River Basin, which supplies water to over 40 million people and over 5.5 million acres of irrigated agricultural land (Deems et al., 2013). Within the basin, the Colorado Basin River Forecasting Center (CBRFC) provides short-term (e.g., 1-2 week lead-time) deterministic forecasts of streamflow and longer-term (i.e., several month lead-time) probabilistic forecasts of snowmelt-driven seasonal runoff volume to regional stakeholders and water resource managers (Bender et al., 2014). CBRFC employs the SNOW-17 temperature-index snow accumulation and ablation model (Anderson, 1976; Anderson, 2006) to simulate the snowmelt contribution to soil infiltration and runoff in the coupled SAC-SMA runoff model. In lieu of explicitly resolving the energy balance at the snow surface for snowmelt simulations, SNOW-17 indexes snowmelt from air temperature and day of year using a suite of tuned model parameters. At each forecast point in the basin, parameters in the SNOW-17/SAC-SMA system are calibrated over a 30-year period based solely on comparisons between modeled and observed streamflow, a common practice in conceptual runoff modeling.

While this type of calibration maximizes the likelihood of higher model skill during average conditions, the problem is that it is prone to failure during years with unusual snow or hydrologic conditions (Seibert, 2003). As a primary example, Bryant et al. (2013) linked streamflow forecasting errors with changes in the radiative forcing of dust-on-snow in four headwater catchments of the San Juan Mountains in southwest Colorado. The greatest model errors were in high and low dust years. Forecast errors were minimized during years with average dust-on-snow radiative forcing, implying that the model calibration period included a mix of clean and dusty snow years. These findings highlight that year-to-year variations in snow conditions and the surface energy balance can change the relationship between snowmelt and air temperature, thereby eroding the utility of index-based models like SNOW-17 in unusual conditions. Beyond dust-on-snow, a variety of factors can lead to spatial and annual variations in energy availability, such as maximum snowpack accumulation and the magnitude of spring snowstorms. Maximum snowpack accumulation is a controlling factor in the timing of the spring snowmelt season and the synchronization with maximum energy availability (Trujillo & Molotch, 2014). Occurrence of spring snowstorms can expand the snowmelt season by providing additional mass to the snowpack, changing the springtime radiation climate (e.g., cloudy and longwave-enhanced vs. clear and shortwave pronounced), and increasing snow albedo, reducing net shortwave inputs. Hence, multiple climatic factors influence how well SNOW-17 represents snowmelt.

Paper presented Western Snow Conference 2016
[1] Cooperative Institute for Research in Environmental Sciences (CIRES) / National Snow and Ice Data Center (NSIDC) / Western Water Assessment (WWA), University of Colorado, Boulder, 80309, mraleigh@nsidc.org

To improve operational resiliency against unusual snow conditions, modifications to the snowmelt CBRFC modeling practices are necessary. Possible approaches include modifications to (1) the SNOW-17 parameters, (2) the SNOW-17 forcing data, and (3) the snow model structure (i.e., select a different snow model). This study presents initial investigations into changing SNOW-17 parameters with the goal of understanding how melt parameters vary spatially and annually across the Upper Colorado River Basin (UCRB) domain. Ongoing efforts from the CBRFC and their collaborators are examining whether changing the SNOW-17 temperature data (e.g., to compensate for the influence of dust-enhanced snowmelt) or selecting more physically based snow models reduces vulnerability to degraded forecasts under unusual dust-on-snow conditions. Here, we use data from 110 NRCS snow telemetry (SNOTEL) stations across a 30-year period (water years 1985-2014) to estimate SNOW-17 parameters spatially and annually, and to examine their linkages between dust, peak snow water equivalent (SWE), and spring snowfall and temperature. While we consider all snow parameters in the experiment, our focus is on the maximum melt factor (MFMAX) parameter because it strongly controls spring snowmelt rates.

OVERARCHING FRAMEWORK AND EXTENDED BACKGROUND

A coherent framework for classifying the influence of multiple climatic factors on streamflow in the UCRB was presented in the "dust enhanced runoff" typology of Landry & Buck (2014). Their typology considers three characterizing variables, each with three categories: winter snow accumulation (i.e., low, average, and high March 1 snow water equivalent), spring weather (dry, average, and wet), and dust loading (minimum, average and maximum). This design allowed for as many as 27 (3x3x3) different hydrograph regimes that could be produced based on these climatic factors. While this typology was useful for classifying recent years in the UCRB, Landry & Buck (2014) considered it a tool for retrospective watershed analysis and not for streamflow forecasting. However, we suggest that the typology could be relevant in a forecasting context if a set of model parameters was identified for each hydroclimatic regime in the typology. This type of approach would yield a library of model parameters, whereby an ensemble of simulations (as a function of the parameter library) could be used to forecast streamflow. Specific ensemble members could be weighted more strongly depending on knowledge of current basin conditions. In order to realize this proposed methodology in the UCRB, a quantitative understanding of the connections between SNOW-17 parameters and multiple climatic factors (i.e., dust-on-snow, peak snow conditions, spring temperature, and spring snowstorms) is needed. Additionally, spatial and annual variations of these linkages must be assessed.

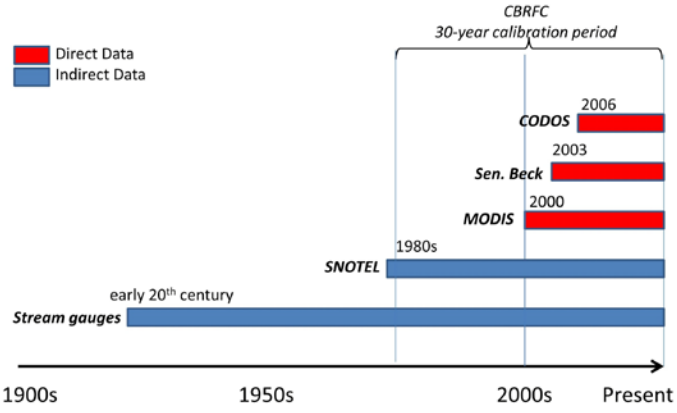

Figure 1. Chronology of datasets in the Upper Colorado River Basin. Datasets are colored based on whether they provide direct or indirect information about dust-on-snow conditions. The 30-year CBRFC calibration period is shown for reference.

Classifying individual water years into the above typology requires knowledge about specific snow, weather, and dust conditions during each year and their spatial variations across the basin. While annual snow accumulation and spring snowstorms dynamics can be gleaned through snow data (e.g., SNOTEL snow pillows) and streamflow observations, there is a distinct lack of comprehensive dust data for construction of the typology. Extensive quantitative datasets of dust-on-snow in the UCRB extend only back to the early 2000s (Figure 1). This includes manual and *in situ* observations from the Colorado Dust on Snow (CODOS) program and Senator Beck Basin (Skiles et al., 2012; Painter et al., 2012a; Landry et al., 2014), and remotely sensed dust radiative forcing from MODIS (Painter et al., 2012b).

While direct monitoring of dust-on-snow in the UCRB ramped up in the early 2000s and garnered considerable attention from the scientific and forecasting communities, the dust-on-snow phenomenon is not new to the region. Lake sediment records suggest that the southwestern United States is prone to natural dust events, though enhanced levels of dustiness have prevailed over the last ~150 years, coincident with westward expansion and settlement of the United States (Routson et al., 2016). Sediment records can resolve decadal variability but are unable to provide clues about annual variability in dust loading, and are therefore not directly useful for this analysis. Accounts in local newspapers and scientific journals provide anecdotal evidence of historic dust-on-snow

events. For example, Harris A. Jones (1913) reported in the *Monthly Weather Review* a wet deposition event in mid-March 1913 that delivered 3.2 mm (0.125 inches) of dust with 22.6 cm (8.9 inches) of snowfall near Wagon Wheel Gap (San Juan Mountains). In early February 1932, an article in *The Steamboat Pilot* documented a wet dust deposition event that brought an estimated 23 g m^{-2} of red dust with 5 cm of new snowfall to Durango ("Snowed red soil in Durango storm", 1932). The level of dust loading reported in this February 1932 storm is comparable to the largest single dust event recorded at the Swamp Angel Study Plot (Senator Beck Basin) from 2010-2013 (Skiles et al., 2015). While we lack comprehensive knowledge about the seasonal to annual dust conditions in the historic record, anecdotal evidence confirms that significant individual dust events indeed occurred in the UCRB prior to the 2000s.

To summarize: (1) our framework requires specific knowledge of dust levels across the UCRB each year in the CBRFC 30-year calibration period, (2) we lack long-term datasets with quantitative dust information before the year 2000, and (3) multiple strands of evidence suggest that dust-on-snow events occurred prior to expanded observations in the 2000s. The question arises, "Can ancillary datasets reveal anything about annual dust conditions in the UCRB prior to the year 2000?" The primary sources of snow and hydrology data in the basin are SNOTEL snow pillow data and USGS streamflow gauges, respectively. In this analysis, we attempt to link operational snow model parameters to annual variations in dust, snow accumulation, and spring snowfall, as inferred from SNOTEL data. The central idea of our study is that the integrated use of SNOTEL data and the SNOW-17 model in the UCRB can provide quantitative linkages between melt dynamics and climatic factors during the period with observed dust data (2000s to present), and therefore can offer clues about dust conditions prior to the year 2000.

DATA

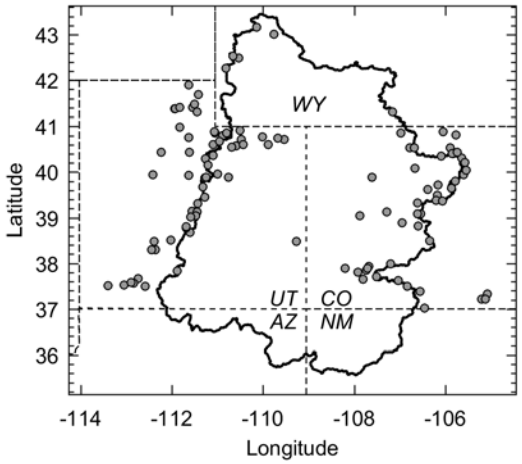

Figure 2. The 110 SNOTEL sites included in the analysis. The black solid line is the boundary of the UCRB while dashed lines are state boundaries.

We conducted the analysis using daily SWE and air temperature data from NRCS SNOTEL sites (Serreze et al., 1999) in the UCRB region. Our study region included sites that were located in Colorado or Utah (some outside of the UCRB) or within the UCRB boundary in Wyoming. We started with 215 SNOTEL sites in this domain, and then checked the availability of daily SWE and air temperature data at each site, retaining only sites with complete data spanning water years (WY) 1985-2014. Mean daily air temperature data were obtained from the corrected station dataset of Oyler et al. (2015) to reduce systematic errors and inhomogeneity in the temperature dataset (Rangwala et al. 2015). While we did not assume these corrections removed all errors from the temperature data, we considered the corrected dataset an improvement over the raw temperature data. After screening for quality and completeness of data, 110 of the 215 stations remained for analysis (Figure 2). For our experiment, we did not use SNOTEL precipitation data, and instead inferred precipitation from changes in SWE with corrections applied within the model calibration. We used this approach to avoid inconsistencies between measured precipitation and SWE, and reasoned this was valid in a region where most winter precipitation is snowfall. Furthermore, our analysis was constrained to the snow season, as reported directly from observed SWE at each snow pillow.

SNOW MODEL

We used the SNOW-17 snow accumulation and ablation model (Anderson, 1976; Anderson, 2006) configured at the point scale for simulations of snowpack development and melt at each of the 110 SNOTEL sites across the 30-year period. As noted in the introduction, this is the same snow model used in operational streamflow forecasting at the CBRFC, although the CBRFC runs the model in a lumped configuration over elevation zones in each sub-catchment of the UCRB. Because the current study is oriented at the point scale, the results are relevant to CBRFC operations in a conceptual sense. The model includes 12 parameters, half of which are considered major parameters (Anderson, 2006). We only consider eight parameters in our calibration experiment (see next section),

based on knowledge about the relative importance of the parameters and the overall model sensitivity (He et al., 2011; Franz & Karsten, 2013). The description and ranges of these parameters are listed in Table 1.

The model simulates snow accumulation, accounts for cooling of the snowpack via a heat deficit concept, and computes snowmelt differently for non-rain periods vs. rain-on-snow events (not included here). A complete description of these routines can be found in Anderson (2006). Of specific interest to this study is how the model computes snowmelt during non-rainy periods, when net radiation likely contributes more energy than turbulent fluxes to snowmelt. The model computes snowmelt from air temperature and a seasonally varying melt factor:

$$Melt = MF_i \times (T_{air} - MBASE) \tag{1}$$

where *Melt* is daily snowmelt (mm), MF_i is the melt factor (mm °C^{-1} d^{-1}) on a given day, T_{air} is mean daily air temperature (°C), and *MBASE* is a parameter that specifies that threshold temperature (°C) for melt conditions. The daily melt factor varies seasonally with a sinusoidal curve, with the maximum melt factor specified with parameter MFMAX on the summer solstice (fixed at June 21) and the minimum melt factor specific with parameter MFMIN on the winter solstice (fixed at December 21):

$$MF_i = \left(\frac{\Delta t}{6}\right)\left\{\left(0.5 \times \sin\left(\frac{2\pi N}{366}\right) + 0.5\right)(MFMAX - MFMIN) + MFMIN\right\} \tag{2}$$

where Δt is the model timestep (hrs) and *N* is the day number since the spring equinox (fixed at March 21). In our study, a timestep of 24 hours was used. When the air temperature is less than MBASE (equation 1), the melt factor curve (equation 2) has no immediate consequence to computed snowmelt.

Table 1. SNOW-17 model parameters adjusted in this study and the ranges of each parameter considered.

Parameter	**Description**	**Units**	**Range**
MFMAX	Maximum melt factor	mm °C^{-1} 6 h^{-1}	[0.50, 3.00]
MFMIN	Minimum melt factor	mm °C^{-1} 6 h^{-1}	[0.05, 0.50]
MBASE	Melt threshold temperature	°C	[-1.0, 1.0]
SCF	Snowfall correction factor for gauge undercatch or drifting snow	--	[0.70, 1.40]
UADJ	Average wind function for rain-on-snow events	mm mb^{-1}	[0.0, 0.2]
TIPM	Antecedent temperature index	--	[0.1, 1.0]
NMF	Maximum negative melt factor	mm °C^{-1} 6 h^{-1}	[0.05, 0.50]
PLWHC	Maximum liquid water hold capacity	fraction	[0.02, 0.30]

METHODOLOGY

Prior studies have utilized SNOTEL data to compute melt factors (equation 1) by comparing cumulative snowmelt (from SWE) to cumulative temperature values above the melt threshold (i.e., positive degree-days). For example, DeWalle et al. (2002) calculated melt factors from seven SNOTEL sites in the Upper Rio Grande Basin over a five year period, and found that melt factors were lowest during the year with the lowest snow accumulation. Likewise, Raleigh & Clark (2014) computed annually varying melt factors from 510 SNOTEL stations across the western USA and found that melt factors decreased with decreasing peak SWE at over 90% of the sites. Concepts related to energy availability help explain these relationships. First, peak SWE magnitude is positively correlated with the timing of the snowmelt season, the date of snowpack disappearance, and seasonally averaged snowmelt rates (Trujillo & Molotch, 2014). Hence, lower snowpack accumulation leads to a shift in the snowmelt season to earlier in the year when energy availability is lower, resulting in lower snowmelt rates. Second, the relative importance of solar radiation vs. sensible heat flux is controlled in part by the timing of the snowmelt season, and these two energy terms exhibit diverging relationships with melt factors (Hock, 2003). Enhanced absorption of solar radiation, whether through increasing insolation (with later snowmelt) or declining snow surface albedo (e.g., aged snow grains or dust/impurity loading at the surface), leads to higher melt factors. In contrast, enhanced sensible heat flux is associated with lower melt factors because information in air temperature is implicitly included in that flux. The surface energy balance is usually not measured but is coupled with melt factor variations, which can be derived

from SNOTEL observations. The implication is that annual and spatial variations in the energy balance regime, in a relative sense, can be inferred from melt factors at SNOTEL sites.

To make the analysis more directly relevant to the CBRFC, we employed a methodology that integrated the SNOW-17 model into the exploration of melt factors across the UCRB (rather than computing these directly from SNOTEL data). Our approach was a year-specific and station-specific calibration of SNOW-17 over the 30-year study period and 110 SNOTEL stations. At each station and year, we selected 5000 parameter sets with random parameters sampled in the range of each of the eight SNOW-17 parameters (Table 1). For each parameter set, we ran SNOW-17 and then computed the root mean squared error (RMSE) between observed and modeled snowmelt time series. After repeating for all 5000 parameter sets, we identified the top 1% (n=50) simulations with the lowest RMSE in snowmelt, and then computed the average parameter value of all eight SNOW-17 parameters for those "best" simulations. This was repeated for all 30 years and all 110 SNOTEL stations. The result was a 3-dimensional dataset of size 30x110x8 that described the "optimal" eight model parameters (Table 1) in space (110 SNOTEL sites) and time (30 years). While more sophisticated optimization routines are available (e.g., Duan et al., 1993), we selected this approach because of its computational efficiency.

After deriving the "optimal" model parameters, our focus was on the MFMAX parameter and its variations in space and time in the UCRB. The MFMAX parameter is a critical SNOW-17 parameter for spring snowmelt, coincident with the dominant timing of dust-on-snow events in the UCRB (Painter et al. 2012a). In addition to year-specific and site-specific MFMAX values, we examine the long-term mean MFMAX and coefficient of variation (CV, the ratio of the standard deviation to the mean) across all stations. To facilitate comparisons of MFMAX between sites, years, and other variables, we converted MFMAX to z-scores (i.e., anomalies) at each site:

$$Z = \frac{x - \mu}{\sigma} \tag{3}$$

where μ is the mean of x and σ is the standard deviation of x. A z-score (Z) of +1.0 indicates that particular value is one standard deviation above the mean. At each station and year, we also calculated peak SWE, total snowfall in the spring (i.e., from peak SWE to the first snow-free date), and mean spring air temperature, and then converted these to z-scores for comparisons with MFMAX. We defined the spring season based on the SWE data at each site/year; spring was the period from the date of peak SWE to the first snow-free date after peak SWE. This was defined to coincide with the period that is characterized primarily by snowmelt. While there are other ways of defining the spring season (e.g., fixed date from the spring equinox to melt-out or to the summer solstice), initial comparisons suggested these other approaches did not yield drastically different results. For quantitative dust data, we compared MFMAX at select sites in the San Juan Mountain Range to dust concentrations measured at the Swamp Angel Study Plot over 2005 to 2013 (Skiles et al., 2015).

RESULTS

Spatial and Interannual Variability in Melt Factors

We first examined the patterns in the maximum melt factor (MFMAX) parameter in terms of the long-term mean and the coefficient of variation (Figure 3a). Long-term mean MFMAX ranged from 0.56 to 1.6 mm $°C^{-1}$ 6 h^{-1} across the sites, with notably high values found in the southeastern part of the basin (i.e., the San Juan Mountain range) and with lower MFMAX values occurring to the north. The interannual variability in MFMAX, as represented with the coefficient of variation (CV), ranged from 2.2 to 37% (Figure 3b). A subtle latitudinal gradient in MFMAX interannual variability was found (particularly along the eastern part of the domain), with southern sites generally having higher year-to-year variability in MFMAX than northern sites.

Correlations between MFMAX and geophysical parameters (i.e., latitude, longitude, elevation, and canopy closure) were generally weak but in some cases were statistically significant (Table 2). First, MFMAX mean and variability were both negative related to latitude with statistical significance ($p<0.01$). Second, the long-term mean MFMAX had a significant ($p<0.05$), albeit weak, negative relationship with canopy closure. The relationship with canopy closure may be somewhat underrepresented because the imprecise GPS coordinates of the SNOTEL sites were used (from NRCS public metadata), and these were used to extract data from a relatively coarse (30 m) canopy cover map. Given that our MFMAX values were derived at the scale of a snow pillow, we expect that local

physiographic factors (i.e. 1 to 5 m) may dominate the snowmelt dynamics at each SNOTEL site, and these were not represented well with the available forest and spatial coordinate data.

The greatest correlation found in our analysis was between mean MFMAX and the CV of MFMAX (r=0.71, p<0.01). This result indicated that sites with higher long-term mean MFMAX also tended to have higher year-to-year variability in MFMAX. This can be seen in time series from two examples sites in different parts of the study domain (Figure 3c). The Red Mountain Pass site from the San Juan Mountains (southern domain) had high values in terms of both mean (0.98 mm $°C^{-1}$ 6 h^{-1}) and CV (21%) in MFMAX. In contrast, a site to the north, Hoosier Pass, had low mean (0.62 mm $°C^{-1}$ 6 h^{-1}) and low CV (8%) in MFMAX. Notable anomalies in MFMAX corresponded between these sites in some years (e.g., water year 2010) but not others (e.g., water year 1991). In addition, the domain-mean MFMAX did not always correspond to the large annual anomalies in MFMAX at sites like Red Mountain Pass. These results suggested that unusual snow conditions did not always setup uniformly across the basin and that sub-regions may exhibit contrasting snowmelt conditions in a given year.

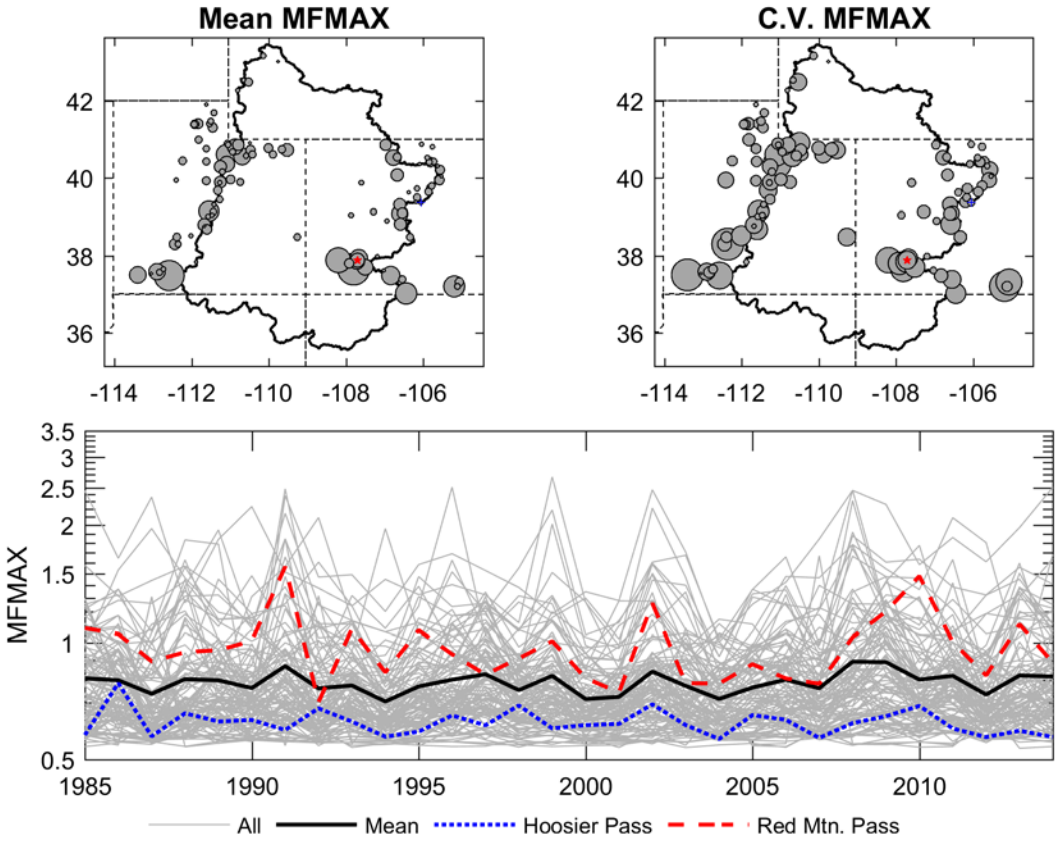

Figure 3. (top) Spatial patterns in the mean and coefficient of variation (CV) in the maximum melt factor (MFMAX) derived with the SNOW-17 calibration experiment at 110 SNOTEL sites over WY 1985-2014 in the UCRB region. The size of the circles are scaled relative to the magnitude of the mean and CV of MFMAX. (bottom) Annual variations in MFMAX across the SNOTEL sites in the UCRB domain. Shown are all sites, the mean across all sites, and individual time series at a site with low mean and low variability in MFMAX (Hoosier Pass) and at a site with high mean and high variability in MFMAX (Red Mountain Pass). Note the y-axis is a log scale.

Table 2. Correlation coefficients between MFMAX (long-term mean and CV) and other geophysical factors across the 110 SNOTEL sites (* signifies a p-value <0.05 while ** signifies a p-value < 0.01).

	Latitude	Longitude	Elevation	Canopy Closure	CV MFMAX
Mean MFMAX	-0.36**	0.02	-0.15	-0.21*	0.71**
CV MFMAX	-0.42**	-0.06	-0.07	-0.14	--

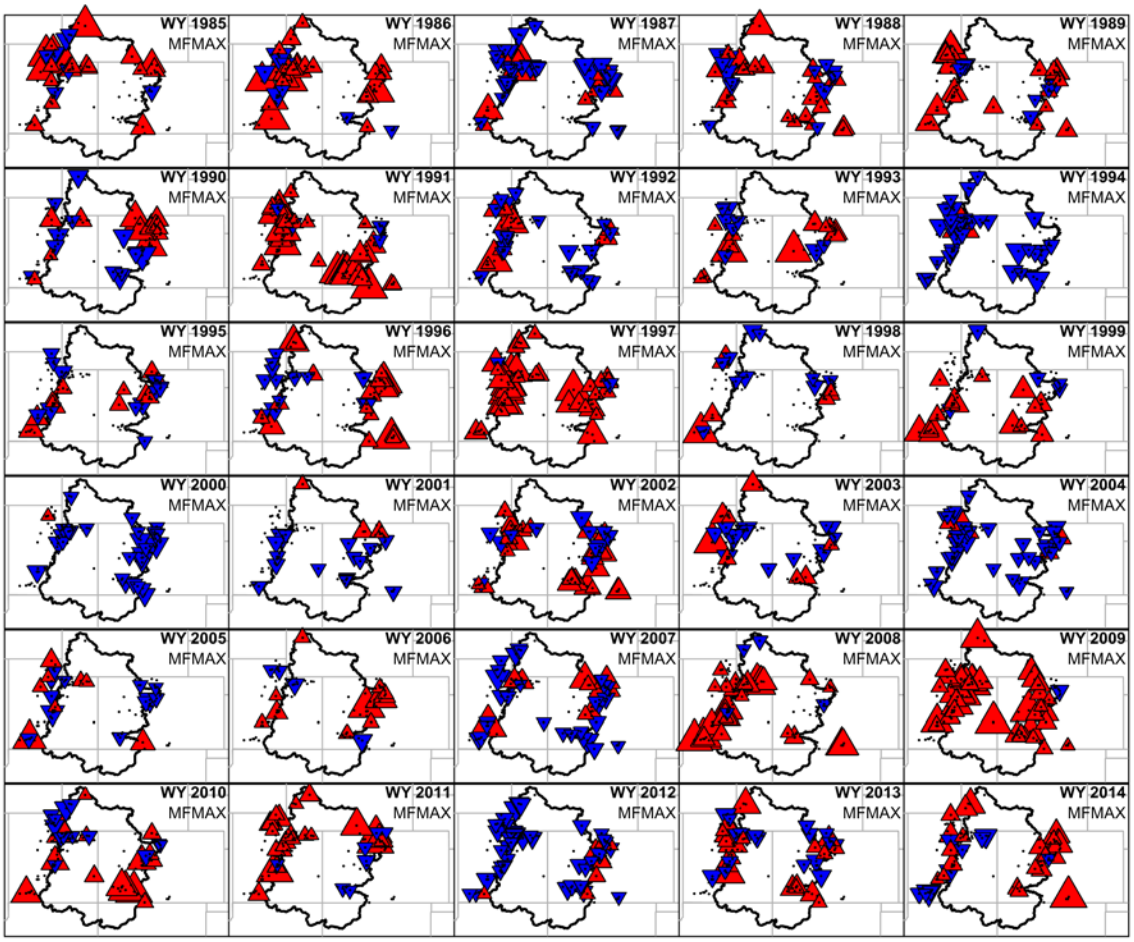

Figure 4. Anomalies in MFMAX across the 110 SNOTEL sites by water year. Red upward-pointing triangles are positive anomalies, blue downward-pointing triangles are negative anomalies, and triangles are sized relative to the absolute value of the anomaly. Cases where the MFMAX anomaly is within one standard deviation of the site mean are plotted as small black dots.

Spatial plots of annual MFMAX anomalies (Figure 4) broadly illustrated similar year-to-year responses across the UCRB domain. Negative MFMAX anomalies were prevalent across the study domain during WY 1994, 2000, and 2012. Positive MFMAX anomalies were common across the sites during WY 1991, 1997, and 2009. However, the strength and sign of the anomalies between sub-regions varied in some years. For example, the western side of the domain had generally consistent positive anomalies during WY 2011 while the eastern side was a mixture of neutral, negative, and positive anomalies. Likewise, sites in the southeastern part of the domain (e.g., the San Juan Mountain region) had MFMAX anomalies that were not consistently linked to anomalies in other sub-regions. MFMAX values were near normal in the San Juan region during WY 1995-1997, despite higher anomalies in the mountain ranges just to the north. The San Juan region also had much stronger anomalies during certain years (e.g., WY 1991, 2002, and 2010), compared to other nearby sub-regions. These results implied that optimal model parameters vary annual and regionally in the UCRB, and hence static snow parameters developed over long time periods and large spatial domains may lead to model vulnerabilities.

Links Between MFMAX Variations and Snowmelt Conditions

Next, we examined linkages between MFMAX variations and conditions relevant to the snowmelt period, including peak SWE, spring snowfall, and mean spring temperatures (Figure 5). At 77 of the 110 sites (70.0%), MFMAX was positively related to peak SWE, and 46 of those sites had a statistically significant ($p<0.05$) relationship. These positive relationships were broadly distributed across the basin (Figure 5), with more consistency on the western part of the domain and a notable absence of correlations between MFMAX and peak

SWE in the San Juan Mountain range area. It should be noted that the magnitude of peak SWE was positively correlated to the timing of peak SWE at 108 of the 110 sites (significant at 82 sites), and hence the link between peak SWE and MFMAX was in part due to the timing of the melt season. MFMAX was inconsistently correlated to spring snowfall, with 66 of the 110 sites having negative relationships and only 6 sites having a statistically significant relationship (regardless of sign) with spring snowfall. Spatially, these relationships exhibited no coherent pattern. Finally, MFMAX was negatively correlated to mean spring temperatures at 86 of the 110 sites (78%), but this was statistically significant at only 36 of the sites. The negative relationship between MFMAX and spring temperatures was more prevalent in the eastern half of the UCRB domain than the western half, with stronger correlations found at sites in the southeast (e.g., San Juan Mountain area).

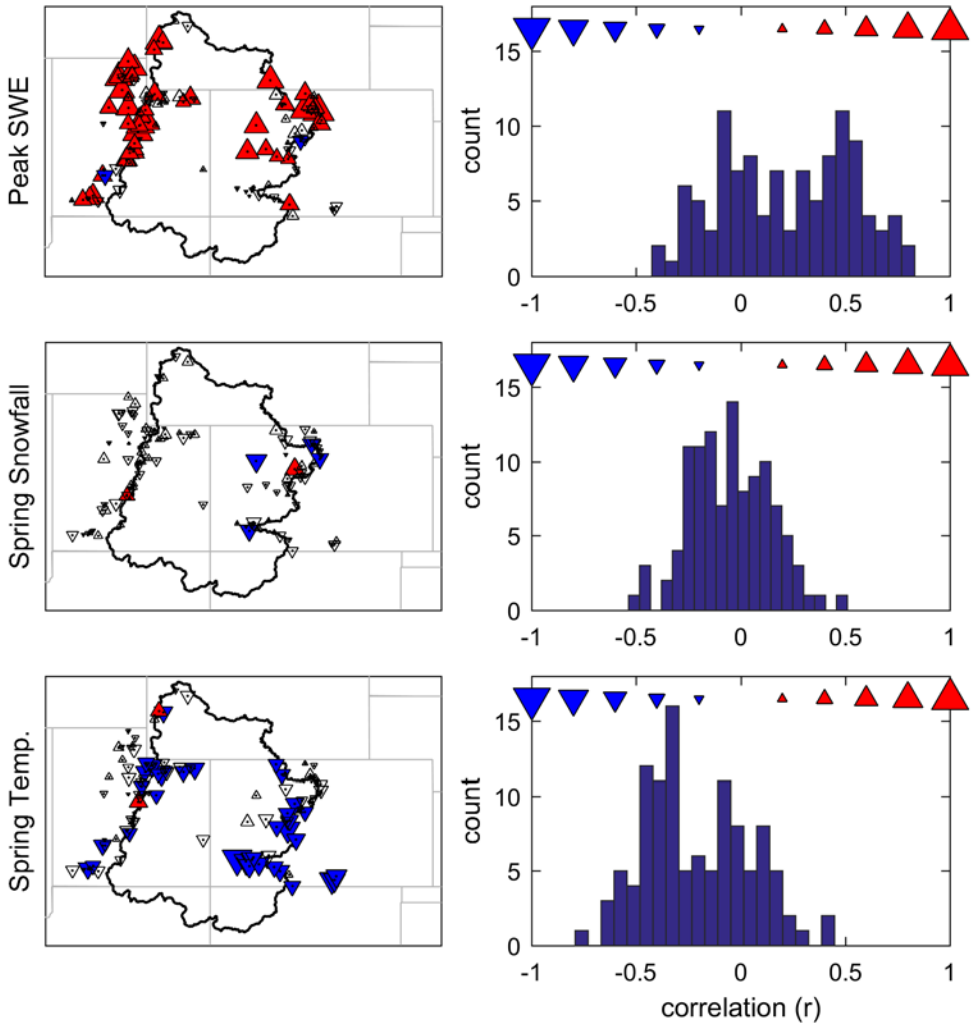

Figure 5. Correlations between MFMAX and (top) peak SWE, (middle) spring snowfall, and (bottom) mean spring (melt season) temperature at the 110 study sites. The spatial mapping of the correlation coefficients are shown on the left, with downward-pointing triangles representing negative correlations, upward-pointing triangles representing positive correlations, colored triangles indicating statistical significance ($p<0.05$), white triangles showing no statistical significance, and the size of the triangle scaled according to the correlation value. The right side shows the corresponding histogram and the scale values of the spatial markers. Here spring snowfall is defined as the total snowfall from peak SWE to snow disappearance, relative to peak SWE. Spring temperature is the mean air temperature from peak SWE to snow disappearance.

Links Between MFMAX Variations and Dust Conditions

To examine connections between MFMAX and quantitative dust data, we focus the analysis on seven SNOTEL sites in the San Juan Mountain range area, where recent dust-on-snow events have been studied in detail.

For context, the anomalies in MFMAX, peak SWE, spring snowfall, and spring temperature at these sites over the 30-year period are shown in Figure 6. The seven sites exhibited similar year-to-year variations in MFMAX, with notable positive anomalies in water years 1991, 2002, 2009, 2010, and 2013. Negative anomalies in MFMAX were less prominent than the positive anomalies, but were still noticeably present in water years 1990, 2000, and 2001. Across the 30-year period, the mean MFMAX anomaly (averaged across the seven sites) was not significantly correlated to peak SWE or spring snowfall, but was significantly correlated to spring temperature ($r = -0.73$, $p<0.01$). This negative correlation with spring temperature suggested that higher MFMAX values arise in cooler conditions during the snowmelt season. Quantitative dust concentration data were collected at the Senator Beck Basin and data from WY 2005-2013 were presented by Skiles et al (2015) and showed WY 2009, 2010, and 2013 as years with high dust concentrations (see red highlighted regions in Figure 6). The correlation between MFMAX and the dust concentration data (not shown) over 2005-2013 was statistically significant ($r=0.88$, $p<0.01$), thereby suggesting a link between dust conditions and snowmelt dynamics (as represented with MFMAX in our experiment).

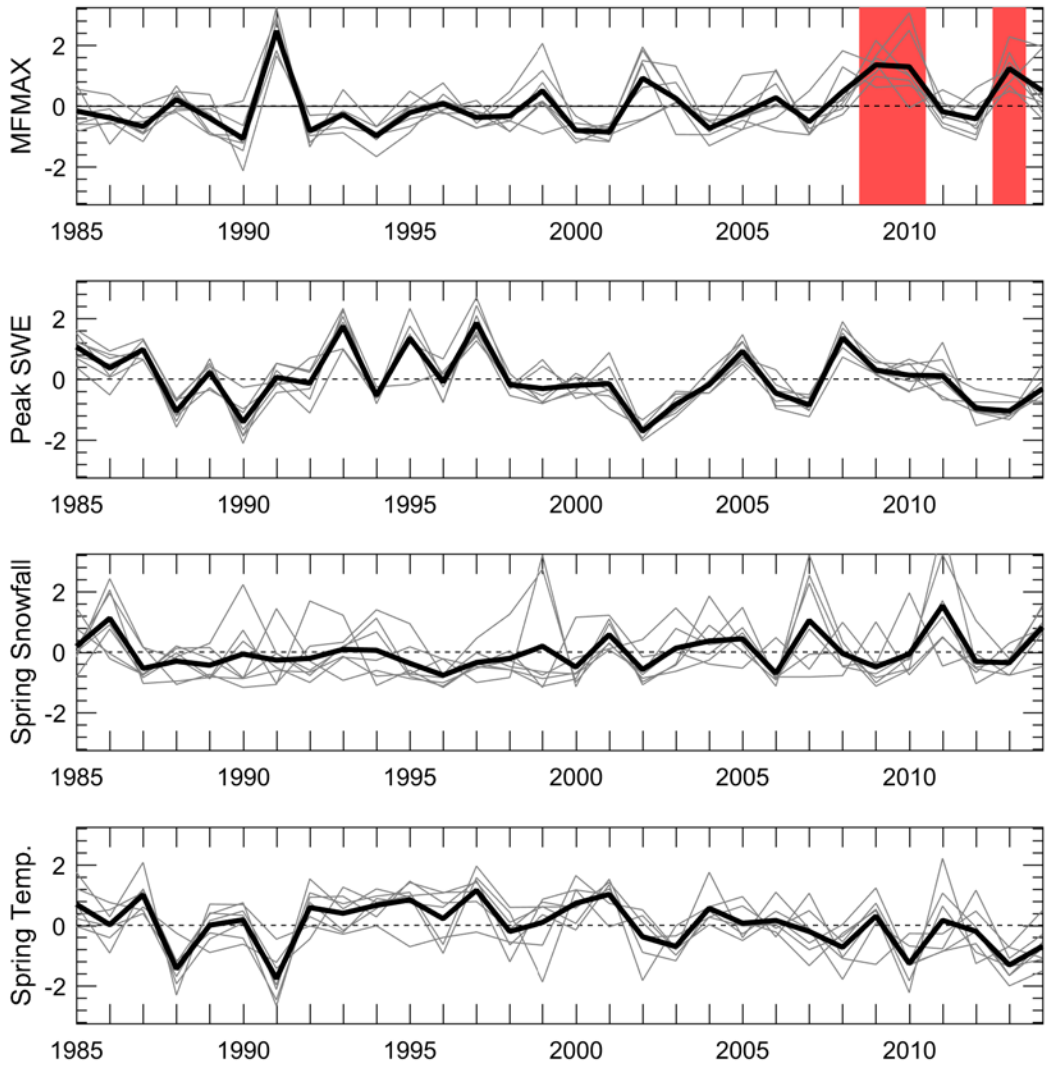

Figure 6. Annual anomalies (z-scores) in MFMAX, peak SWE, spring snowfall, and spring temperature at seven SNOTEL sites (Beartown, Cascade, Idarado, Lizard Head Pass, Lone Cone, Mineral Creek, Red Mountain Pass) in the San Juan Mountain sub-region. The gray lines are the individual seven SNOTEL sites while the black line is the mean of the seven sites. The red highlighted regions in the top panel are known heavy dust years based on concentration data observed over 2005-2013 at Senator Beck (Skiles et al., 2015). See the caption of Figure 5 for definitions of spring snowfall and temperature.

DISCUSSION

The analysis demonstrated that in the UCRB domain, the optimum maximum melt factor (MFMAX) parameter varies both spatially and annually. Of the variables considered in the correlation analysis, MFMAX was most frequently correlated with peak SWE (positive) and spring temperatures (negative). The linkage with peak SWE found here was different from what has been found in some studies with SNOTEL data. For example, He et al. (2011) reported that MFMAX was weakly related to peak SWE and found a negative (rather than positive) relationship. The inconsistency in these results may be due to the fact the we considered a single hydroclimate whereas He et al. (2011) examined SNOTEL sites from across the western USA. Our results are congruent with the results of DeWalle et al. (2002) and Raleigh & Clark (2014), who found positive relationships between peak SWE and melt factors. Peak SWE influences overall melt efficiency (as reflected in the MFMAX parameter) by controlling the timing of the snowmelt season.

The analysis in the San Juan Mountain region established opposing linkages between MFMAX and spring temperature (negative relationship) versus MFMAX and dust concentration (positive relationship). Absolute values of these correlations were of similar magnitude, which raises the question, "which factor, temperature or dust, is responsible for the MFMAX variations?" While the adage "correlation does not imply causation" certainly holds in the context of our experimental design, a plausible physical explanation is that dust is the driver of variations in both MFMAX and spring temperature. Earlier snowmelt from dust-enhanced melt drives the snowmelt season to earlier in the year, when temperatures are cooler. This also shifts the energy balance more towards shortwave radiation melt (due to lower albedo and higher shortwave absorption), which is associated with higher melt factors (Hock 2003). We assume rather than demonstrate these relationships; future work will examine correlations between dust-enhanced snowmelt, the surface energy balance, and spring temperatures in more detail.

Our analysis implied a new way of using MFMAX to detect years in the historical record that may have had enhanced dust-on-snow conditions. As a prime example, WY 1991 had the highest MFMAX anomaly across the seven SNOTEL sites in the area, but quantitative data on dust conditions were not available in that year (Figure 1). However, anecdotal evidence from a Space Shuttle photograph (Figure 7) suggests that dust-on-snow conditions prevailed in the San Juan Mountains in the 1991 melt season. Coincidentally, the spring air temperature had a strong negative anomaly that year. Without dust data, this temperature anomaly might otherwise suggest that MFMAX had to be higher to account for melt under colder spring conditions. It is also possible that a negative temperature anomaly arises in dust-influenced snow years, as the dust shifts the snowmelt season earlier in the year when the climate is cooler (recall that we defined spring based on the period from peak SWE to snow disappearance). This is evident in recent years when we had quantitative dust knowledge, such as water years 2010 and 2013 (Figure 6). However, certain years do not fit this pattern, such as the notoriously dusty water year 2009.

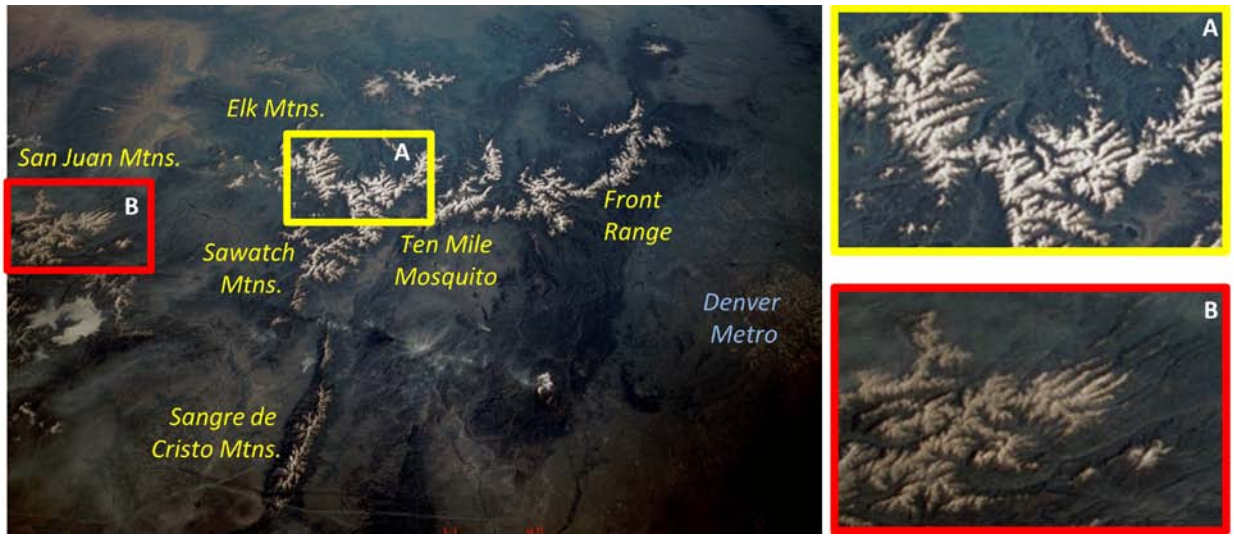

Figure 7. Photograph of Colorado mountain ranges in June 1991 from the Columbia Space Shuttle (Mission STS-040). Panels A and B are zoomed to show visible differences in the snowpack of the Sawatch/Elk Mountain area vs. the San Juan Mountains. Photo: NASA Gateway to Astronaut Photography of Earth (http://eol.jsc.nasa.gov).

SUMMARY

The analysis demonstrated how data from SNOTEL sites can be paired with an operational snow model to gain knowledge about spatial and interannual variability in optimal snowmelt parameters. These parameters can be linked to some geophysical characteristics (e.g., latitude and forest cover) and variations in snowmelt conditions (e.g., peak SWE, dust-on-snow, and spring temperature). Additionally, the approach can be used in a diagnostic sense (Figures 6 and 7) to detect unusual snow conditions in the historic record. Moving forward, the melt factor variations from SNOTEL sites need to be compared to information contained in remote sensing products (e.g., MODDRFS) and streamflow measurements to examine snow conditions over more spatially comprehensive measurement platforms. We expect that SNOTEL, MODIS, and streamflow data have much to teach us about unusual snowmelt conditions in the UCRB. These datasets will be essential for identifying opportunities to improve the operational forecasting system.

ACKNOWLEDGMENTS

The first author was supported by a CIRES Visiting Fellowship and was hosted at the National Snow and Ice Data Center. We would like to thank Stacie Bender and the Colorado Basin River Forecasting Center (CBRFC) staff for helpful discussions and ongoing collaborations on this topic. Additional thanks are due to the many researchers who have been studying recent dust-on-snow events in the Colorado River Basin. In particular, we would like to recognize the contributions of Chris Landry and Annie Bryant for prompting this analysis.

REFERENCES

Anderson, E. 1976. A point energy and mass balance model of a snow cover, NOAA Tech. Rep. NWS 19, Silver Spring, MD.

Anderson, E. 2006. Snow Accumulation and Ablation Model–SNOW-17.

Anonymous. 1932. Snowed red soil in Durango storm, The Steamboat Pilot, 5th February, 3.

Bender, S., P. Miller, B. Bernard, and J. Lhotak. 2014. Use of snow data from remote sensing in operational streamflow prediction, Proc. 82nd Western Snow Conference, pp. 79–89, Durango, CO.

Bryant, A. C., T. H. Painter, J. S. Deems, and S. M. Bender. 2013. Impact of dust radiative forcing in snow on accuracy of operational runoff prediction in the Upper Colorado River Basin, Geophys. Res. Lett., 40, 3945–3949, doi:10.1002/grl.50773.

Deems, J. S., T. H. Painter, J. J. Barsugli, J. Belnap, and B. Udall. 2013. Combined impacts of current and future dust deposition and regional warming on Colorado River Basin snow dynamics and hydrology, Hydrol. Earth Syst. Sci., 17(11), 4401–4413, doi:10.5194/hess-17-4401-2013.

DeWalle, D., Z. Henderson, and A. Rango (2002), Spatial and temporal variations in snowmelt degree-day factors computed from SNOTEL data in the Upper Rio Grande basin, Proc. 70th Western Snow Conference, pp. 73–81, Granby, CO.

Duan, Q. Y., V. K. Gupta, and S. Sorooshian. 1993. Shuffled complex evolution approach for effective and efficient global minimization, J. Optim. Theory Appl., 76(3), 501–521, doi:10.1007/BF00939380.

Franz, K. J., and L. R. Karsten. 2013. Calibration of a distributed snow model using MODIS snow covered area data, J. Hydrol., 494, 160–175, doi:10.1016/j.jhydrol.2013.04.026.

He, M., T. S. Hogue, K. J. Franz, S. A. Margulis, and J. A. Vrugt. 2011. Characterizing parameter sensitivity and uncertainty for a snow model across hydroclimatic regimes, Adv. Water Resour., 34(1), 114–127, doi:10.1016/j.advwatres.2010.10.002.

Hock, R. 2003. Temperature index melt modelling in mountain areas, J. Hydrol., 282(1-4), 104–115, doi:10.1016/S0022-1694(03)00257-9.

Jones, H. A. 1913. Effect of dust on the melting of snow, Mon. Weather Rev., 41(4), 599, doi:10.1175/1520-0493(1913)41<599a:EODOTM>2.0.CO;2.

Landry, C., and K. Buck. 2014. Dust-on-snow effects on Colorado hydrographs, Proc. 82nd Western Snow Conference, pp. 13–18, Durango, CO.

Landry, C. C., K. A. Buck, M. S. Raleigh, and M. P. Clark. 2014. Mountain system monitoring at Senator Beck Basin, San Juan Mountains, Colorado: A new integrative data source to develop and evaluate models of snow and hydrologic processes, Water Resour. Res., 50(2), 1773–1788, doi:10.1002/2013WR013711.

Oyler, J., S. Z. Dobrowski, A. Ballantyne, A. Klene, and S. Running. 2015. Artificial amplification of warming trends across the mountains of the western United States, Geophys. Res. Lett., (42), 153–161, doi:10.1002/2014GL062803.

Painter, T. H., S. M. Skiles, J. S. Deems, A. C. Bryant, and C. C. Landry. 2012a. Dust radiative forcing in snow of the Upper Colorado River Basin: 1. A 6 year record of energy balance, radiation, and dust concentrations, Water Resour. Res., 48(7), doi:10.1029/2012WR011985.

Painter, T. H., A. C. Bryant, and S. M. Skiles. 2012b. Radiative forcing by light absorbing impurities in snow from MODIS surface reflectance data, Geophys. Res. Lett., 39(17), 1–7, doi:10.1029/2012GL052457.

Raleigh, M. S., and M. P. Clark (2014), Are temperature-index models appropriate for assessing climate change impacts on snowmelt?, Proc. 82nd Western Snow Conference, pp. 45–51, Durango, CO.

Rangwala, I., T. Bardsley, M. Pescinski, and J. Miller. 2015. SNOTEL sensor upgrade has caused temperature record inhomogeneities for the Intermountain West: Implications for climate change impact assessments, Western Water Assessment Climate Briefing, pp. 1-11, Boulder, CO.

Routson, C. C., J. T. Overpeck, C. A. Woodhouse, and W. F. Kenney. 2016. Three Millennia of Southwestern North American Dustiness and Future Implications, edited by L. Zhu, PLoS One, 11(2), e0149573, doi:10.1371/journal.pone.0149573.

Seibert, J. 2003. Reliability of Model Predictions Outside Calibration Conditions, Nord. Hydrol., 34(5), 477–492, doi:10.2166/nh.2003.028.

Serreze, M. C., M. P. Clark, R. L. Armstrong, D. A. McGinnis, and R. S. Pulwarty. 1999. Characteristics of the western United States snowpack from snowpack telemetry (SNOTEL) data, Water Resour. Res., 35(7), 2145–2160, doi:10.1029/1999WR900090.

Skiles, S. M., T. H. Painter, J. S. Deems, A. C. Bryant, and C. C. Landry. 2012. Dust radiative forcing in snow of the Upper Colorado River Basin: 2. Interannual variability in radiative forcing and snowmelt rates, Water Resour. Res., 48(7), W07522, doi:10.1029/2012WR011986.

Skiles, S. M., T. H. Painter, J. Belnap, L. Holland, R. L. Reynolds, H. L. Goldstein, and J. Lin. 2015. Regional variability in dust-on-snow processes and impacts in the Upper Colorado River Basin, Hydrol. Process., doi:10.1002/hyp.10569.

Trujillo, E., and N. P. Molotch. 2014. Snowpack regimes of the Western United States, Water Resour. Res., 50(7), 5611–5623, doi:10.1002/2013WR014753.